Digest Journal of Nanomaterials and Biostructures Vol. 13, No. 1, January - March 2018, p. 49 - 55

SYNTHESIS OF HEXADECYLAMINE CAPPED ZnO NANOPARTICLES USING *BIS*(2-HYDROXY-1-NAPHTHALDEHYDATO)ZINC(II) AS A SINGLE SOURCE PRECURSOR

T. XABA[a*], M. J. MOLOTO[a], N. MOLOTO[b]
[a]*Department of Chemistry, Vaal University of Technology, P/Bag X021, Vanderbijlpark, South Africa*
[b]*School of Chemistry, Wits University, P O Wits, Braamfontein, 2025, South Africa*

Salicyladehyde and 2-hydroxy-1-naphthaldehyde were used as ligands to prepare *bis*(salicylidene)zinc(II) and *bis*(2-hydroxy-1-naphthaldehydato)zinc(II) complexes. The *bis*(2-hydroxy-1-naphthaldehydato)zinc(II) complex was used as a precursor to synthesize zinc oxide nanoparticles via thermal decomposition technique at different temperatures using hexadecylamine (HDA) as a stabilizing agent. The results show that decomposition temperature has a huge effect during the formation of the ZnO nanomaterials. The TEM images of the as synthesized nanoparticles revealed different shapes of the particles as the decomposition temperature was increased from 145 to 190 °C. The diffraction patterns of all ZnO nanoparticles synthesized at various temperatures show hexagonal structures with the lattice parameter of a = b = 3.25 Å and c = 5.20 Å

(Received September 23, 2017; Accepted January 10, 2018)

Keywords: Zinc complexes; hexadecylamine; zinc oxide; semiconductors; nanoparticles.

1. Introduction

Transition metal complexes have been investigated for many years due to their importance in a number of applications as radiation therapeutic, diagnostic and imaging agent. Metal coordination compounds have also been widely used to synthesize nanosize materials which serves as a link between synthetic chemistry and materials science [1]. The metal complexes are also extremely valuable in biological systems as small molecules as drug deliveries in pharmacology, biochemistry, physiology, and nanotechnological processes [2]. Metal oxides nanoparticles play a very important role in many fields of chemistry, physics and materials science [3, 4]. These nanomaterials can display unique physical and chemical properties due to their restricted size and a high density of the edge surface sites. Among group II-VI semiconductor nanomaterials, zinc oxide has attracted considerable attention lately due to its numerous attractive properties. It has been counted within the new-generation semiconductor materials with a wide band gap energy of 3.3eV, and high excitation energy of 60eV [5]. ZnO has been widely explored as fertilizers, plant protection products, water purification, cancer detector, bio-imaging material etc [5-7].

Khalil *et al.* reported the synthesis and characterization of ZnO nanoparticles by thermal decomposition of a curcumin zinc complex. The thermal behaviour of the zinc precursor was studied [8]. Recently, we have reported the synthesis of face centred cubic ZnO and CdO nanoparticles using the thermal decomposition of the metal complex based on the naphthaldehydato ligand in an organic surfactant at high temperature. Each precursor was dissolved in oleyamine and the mixture was injected into hot trioctylphosphine [9].

Salicyladehyde and 2-hydroxy-1-naphthaldehyde are low-cost materials which have been widely examined in the past for a wide range of biological synthesis [10]. In the present study, The preparation of bis(salicylidene) zinc(II) and bis(2-hydroxy-1-naphthaldehydato)zinc(II) complexes is reported. Bis(2-hydroxy-1-naphthaldehydato)zinc(II) complex was then used to synthesize ZnO

* Corresponding author: thokozanix@vut.ac.za

nanoparticles using hexadecylamine (HDA) as a capping molecule via thermal decomposition technique. The precursors were characterized by Fourier transform infrared (FTIR) spectroscopy, elemental analysis, nuclear magnetic resonance (NMR), and thermogravimetric (TGA) analysis. The synthesized ZnO nanoparticles were characterized by ultraviolet–visible spectroscopy (UV-Vis), photoluminescence (PL), X-ray diffraction (XRD), and transmission electron microscopy (TEM).

2. Experimental

2.1. Materials

Zinc acetate dihydrate, 2-hydroxy-1-naphthaldehyde, salicyladehyde, hexadecylamine (HDA), ethanol, methanol, and toluene were reagents purchased from Sigma-Aldrich and were all used without further purification.

2.2. Synthesis of the precursors

The *bis*(2-hydroxy-1-naphthaldehydato)zinc(II) **complex 1** and *bis*(salicylidene)zinc(II) **complex 2** were prepared by methods reported previously [9, 11]. A brief description of each synthesis is given below

2.2.1. Preparation of the metal complexes

In a typical experiment, a 20 mL ethanolic solution of $Zn(Acetate)_2.2H_2O$ (5 mmol) was added into a 20 mL ethanolic solution of 2-hydroxy-1-naphthaldehyde (HNA) (10 mmol) to form a homogeneous solution. The solution was stirred and refluxed at 60 °C for about 1 hr. The precipitate that settled from the solution was centrifuged and washed with ethanol three times. The product was dried in a vacuum oven at room temperature, weighed and characterized. The same procedure was repeated with salicyladehyde instead of HNA.

*$Zn(C_{11}H_6O_2)_2$ (**complex 1**)*
The complex was obtained as a green solid. Percentage yield: *82%. m.pt. 283 - 293 °C. CHNS analysis: Calc.: C, 65.01; H, 3.15; O, 15.00%. Found: C, 64.81; H, 3.10; O, 15.90%. Significant IR bands: v(C=O): 1647 cm^{-1}, v(M-O): 494 cm^{-1}. ^1H NMR δ (ppm): (400 MHz, DMSO-d_6, 295 K): δ = 10.61 (s, 1H, CH), 8.35 (m, 1H, CH), 7.80 (m, 1H, CH), 7.65 (m, 1H, CH), 7.39 (m, 1H, CH), 7.28 (m, 1H, CH), 6.77 (m, 1H, CH). ^{13}C NMR (400 MHz, DMSO-d_6, 296 K) δ (ppm): 191 (C=O), 160 (C-O), 138 (C-H), 135 (C-H), 134 (C-H), 128 (C-H), 127 (C-H), 124 (C-H), 122 (C-H), 118 (C-H), 111 (C-H)*

*$Zn(C_7H_5O_2)_2$ (**complex 2**)*
The complex was obtained as a light yellow solid. Percentage yield: *67%. m.pt. 227 - 238 °C. CHNS analysis: Calc.: C, 54.66; H, 3.28; O, 20.80%. Found: C, 53.99; H, 3.42; O, 20.57%. Significant IR bands: v*(C=O): 1647 cm^{-1}, *v*(M-O): 540 cm^{-1}. *^1H NMR δ (ppm): (400 MHz, DMSO-d_6, 295 K): δ = 9.82 (s, 1H, CH), 7.47 (m, 1H, CH), 7.35 (m, 1H, CH), 6.77 (m, 1H, CH), 6.61 (m, 1H, CH). ^{13}C NMR (400 MHz, DMSO-d_6, 296 K) δ (ppm): 180 (C=O), 160 (C-O), 138 (C-H), 124 (C-H).*

2.3. Synthesis of ZnO nanoparticles

Zinc oxide nanoparticles were prepared by thermal decomposition of $Zn(C_{11}H_6O_2)_2$ (***complex 1***) in hexadecylamine (HDA). In a typical reaction, HDA (5 g) was mixed the zinc precursor (0.5 g) in a two necked flask. The mixture was refluxed and heated to 145 °C under nitrogen environment. The temperature was maintained for one hour and the mixture was allowed to cool to a temperature of about 70 °C. Addition of methanol (30 mL) produced the product which was then separated by centrifugation. The residue was washed three times with methanol and re-dispersed in toluene for characterization.

2.4. Characterization of the precursors and nanoparticles

Microanalysis was performed on a Perkin-Elmer automated model 2400 series II CHN/O analyzer. Infrared spectra were carried out in the range 400–4000 cm^{-1} using a Bruker FTIR tensor 27 spectro-photometer. Thermogravimetric analysis was conducted at a heating rate of 20 °C min^{-1} through a Perkin-Elmer Pyris 6 TGA up to 600 °C in a closed perforated aluminium pan under nitrogen gas. A Perkin-Elmer Lambda 1050 UV/vis/NIR spectrometer was used to attain UV-Vis absorption measurements of the ZnO nanoparticles while photoluminescence properties were analyzed using an Edinburgh Instruments FLS920 spectrofluorimeter. The glass quartz cuvettes with a 1 cm path length were utilized during the analysis using toluene as a solvent. X-ray diffraction studies were achieved on a Bruker AXS D8 diffractometer using Cu-Karadiation. The nanoparticles were mounted flat and scanned between 2θ = 20-90º.

3. Results and discussion

The synthesis of zinc oxide nanoparticles via thermal decomposition using *bis*(2-hydroxy-1-naphthaldehydato)zinc(II) complex is reported. In this work, zinc complexes were obtained by the reaction of the zinc acetate with a hydroxyl naphthaldehyde or salicyladehyde ligand. The overall synthetic procedure is shown in Scheme 1.

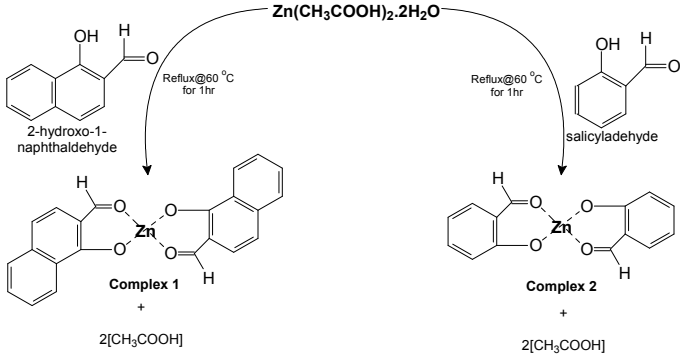

Scheme 1. The preparation of the bis(2-hydroxy-1-naphthaldehydato)zinc(II) complex (1) and bis(salicylidene)zinc(II) complex (2)

Zinc oxide nanoparticles were then synthesized from the decomposition *bis*(2-hydroxy-1-naphthaldehydato)zinc(II) complex in HDA at the temperatures of 145 and 190 °C. The synthesized nanoparticles were analysed by UV-Vis, PL, XRD, and TEM. To understand the performance of semiconductor nanoparticles, the optical absorption study is very important.

3.1. Thermogravimetric analysis (TGA)

The thermal properties of both complexes (1 and 2) were studied by thermogravimetric analysis (TGA) at the temperature ranging from 20 to 600 °C under nitrogen atmosphere. TGA graph for complex 1 in Fig. 1 (a) shows a single step decompositions of the complex with a rapid weight loss between 300 and 350 °C which corresponds to the solid decomposition residue of 61.26 % of the *bis*(2-hydroxy-1-naphthaldehydato) ligand. Whereas, *bis*(salicylidene)zinc(II) complex in Fig 1(b) reveals two step decomposition with a rapid minor weight loss between 90 and 120 °C and a major loss between 250 and 310 °C. The first weight loss may be attributed to the loss of the solvent and the major decomposition temperature is due to the loss of the *bis*(salicylidene) ligand which is confirmed by the percentage loss of 68.31% from the TGA graph.

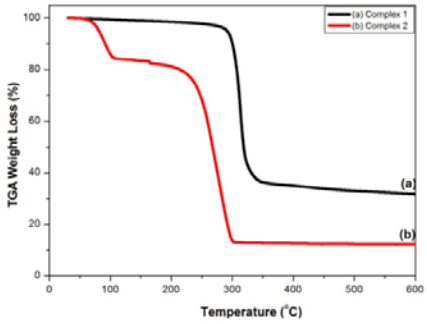

Fig. 1.TGA curves of the bis(2-hydroxy-1-naphthaldehydato)zinc(II) (a) and bis(salicylidene) zinc(II) (b) complexes

3.2. Optical properties

The optical absorption spectrum of ZnO nanoparticles at higher temperature in Fig, 2(b) shows two absorption peaks at 349 nm (3.55 eV) and 387 nm (3.20 eV) whereas at lower decomposition temperature (Fig, 2(b)) reveals only one absorption peak located at 334 nm (3.71 eV) which is blue shifted by 0.41 eV in comparison with the bulk ZnO [12]. The availability of one absorption peak in the spectrum at lower temperature signifies mono-dispersed particles. Band gap energy increases with the decreasing in particle size due to quantum size effects. The band gap can be proposed by Tauc's relationship [13] between the optical absorption coefficient, α, the photon energy (hν), constant (*A*) and the direct band gap energy (Eg) as represented in eqn. (1) below:

$$\alpha h\upsilon = A(h\upsilon - E_g)^n \tag{1}$$

Where n = 1/2 for direct allowed transitions and n = 2 for indirect allowed transition. The plot of $(\alpha h\nu)^2$ against photon energy (hυ) and the extrapolation the linear portion of the curve to absorption coefficient to zero, the Tauc plot in Fig. 2(a) (ii) reveals the estimated band gab energies of 3.82 and 3.65 eV for the nanoparticles synthesized at 145 and 190 °C. The blue shifts in the band edges signify the exciton confinement and also confirm of the presence of nanosized particles.

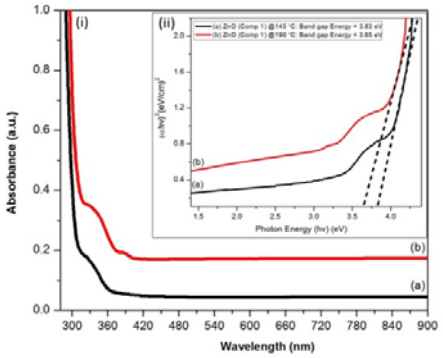

Fig. 2. Absorption spectra (i) and Tauc plots (ii) of HDA capped ZnO nanoparticles synthesized at 145 (a) and 190 °C (b)

Photoluminescence spectrum of ZnO nanoparticles with an excitation wavelength 350nm at room temperature is shown in Figure 3. The emission spectrum of ZnO nanoparticles synthesized at lower temperature (Fig. 3(a)) shows a narrow emission peak located at 399 nm

(3.11 eV). The spectrum of the ZnO nanoparticles prepared at higher temperature (Fig. 3(b)) exhibit two maxima, the strong peak at 409 nm (3.03 eV) and a weak emission peak 431 nm (2.87 eV). The strong emission peak is due to band-to-band transition [11] and the weak peak is due to the single ionized oxygen vacancy in ZnO nanomaterial as well as the reassembling of a photon generated hole with a singly ionized charge of the oxygen vacancy [14-16]. All the obtained results are in agreement with the corresponding absorption spectrum and signify the typical behaviour of ZnO nanocrystals. The emission spectra of the ZnO nanoparticles are red shifted from the absorption spectra and from their bulk ZnO material. The emission peaks shift towards higher wavelength or lower energy when the decomposition temperature is increased during the synthesis of ZnO nanoparticles.

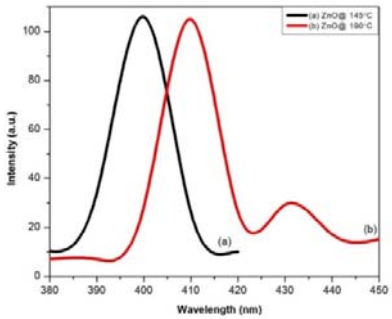

Fig. 3. Emission spectra of HDA capped ZnO nanoparticles synthesized at 145 (a) and 190 °C (b)

3.3. Morphological properties

Figure 4 shows the XRD patterns of the synthesized ZnO nanoparticles at 145 and 190 °C. At higher temperature, the XRD spectrum shows the well-defined multiple diffraction peaks compared to the spectrum at lower temperature due to the presence of some constituencies from the complex during the synthesis of nanoparticles. In both spectra, the peaks that were observed correspond to the (100), (002), (101), (102), (110), (103), (200), (112), (201), (004), and (201) crystalline planes that are well consistent with the structure of ZnO (JCDD 01-076-0704). These XRD patterns could be indexed to hexagonal wurtzite structure which is similar to the reported results by Sun and co-workers [17] with the cell constants of a = b = 3.25 Å and c = 5.20 Å.

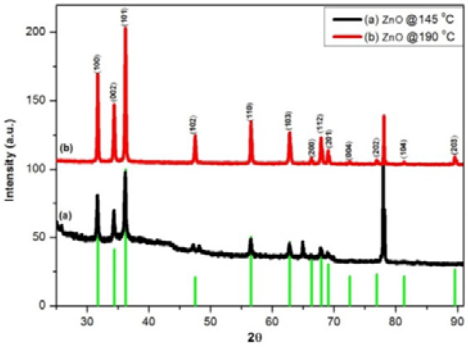

Fig. 4. X-ray diffraction patterns of HDA capped ZnO nanoparticles synthesized at 145 (a) and 190 °C (b)

The size of nanoparticles plays an essential role in controlling the properties of nanomaterials. TEM is a tool that can be used to explore the size, shape and morphology of the particles. The reaction temperature plays an important part during the formation of nanoparticles.

The entire reaction can proceed in either a kinetic or a thermodynamic growth system [18, 19]. The TEM images for ZnO nanoparticles synthesized from *bis*(2-hydroxy-1-naphthaldehydato)zinc(II) complex at the temperatures of 145 and 190 °C are represented in Fig. 5 below.

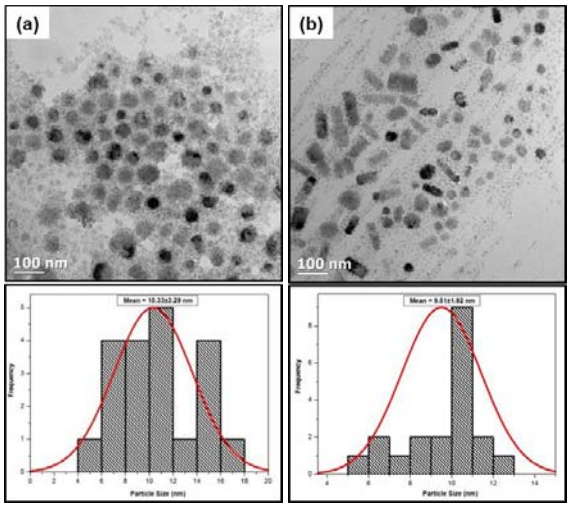

Fig. 5.TEM images and frequency distribution of HDA capped ZnO nanoparticles synthesized at 145 (a) and 190 °C (b)

The TEM results of the ZnO nanoparticles synthesized at the lowest temperature in Fig. 5(a) shows spherical shaped particles that are well defined with an average diameter of 10.33 ± 3.29 nm. Figure 5(b) confirms the combination of spherical, hexagonal and rod-like morphologies. The sizes of spherical and hexagonal ZnO particles were found to be 9.51 ± 1.92 nm while ZnO nanorods were 9.44 ± 2.01 nm in width and 22.34 ± 2.65 nm in length.

4. Conclusions

Zinc complexes have been prepared through simple one step method. The *bis*(2-hydroxy-1-naphthaldehydato)zinc(II) complex has been used as a precursor to synthesize ZnO nanoparticles and thin films. Nanoparticles of ZnO capped with HDA at 190 °C shows two absorption and emission peaks which is a typical behaviour of the ZnO nanomaterial compared to nanoparticles that were synthesized at lower temperature. Spherical and rod-like morphologies of the particles were observed for nanomaterials synthesized at higher temperature whereas spherical particles were formed at lower temperatures. All the nanoparticles prepared at different temperatures exhibit hexagonal phase structured particles.

Acknowledgements

The authors would like to thank the National Research Foundation (NRF), the Vaal University of Technology for funding this project and the University of Manchester for allowing us to use some of their facilities.

References

[1] S. M. Hosseinpour-Mashkani, F. Mohandes, M. Salavati-Niasari, K. Venkateswara-Rao.

Mater Res Bull. **47**, 3148 (2012).
[2] H. Naeimi, Z. Sadat Nazifi, S. Matin Amininezhad, M. Amouheidari, J. Antibiot. **66**, 689 (2013).
[3] J. A. Rodríguez, M. Fernández-García, (Eds.) Whiley: New Jersey. 1 (2007).
[4] M. Fernández-García, A. Martínez-Arias, J. C. Hanson, J. A. Rodríguez, Chem. Rev. **104**, 4063 (2004).
[5] A. Naveed Ul Haq, A. Nadhman, I. Ullah, G. Mustafa, M. Yasinzai, I. Khan, Journal of Nanomaterials. **2017**, Article ID 8510342, 14 pages (2017)
[6] C. Parisi, M. Vigani, and E. Rodríguez-Cerezo, Nano Today. **10**, 124 (2015).
[7] Y. L. Wu, A. I. Y. Tok, F. Y. C. Boey, X. T. Zeng, X. H. Zhang, Appl. Surf. Sci. **253**, 5473 (2007).
[8] M. I. Khalil, M. M. Al-Qunaibit, A. M. Al-zahem, J. P. Labis, Arabian Journal of Chemistry. **7**, 1178 (2014).
[9] T. Xaba, M. J. Moloto, N. Moloto, Asian Journal of Chemistry. **28**, 1015 (2016).
[10] Y. H. Kima, D. K. Lee, B. G. Jo, J. H. Jeong, Y. S. Kang, Colloids and Surfaces A: Physicochem. Eng. Aspects. **284**, 364 (2006).
[11] T. Hyeon, S. S. Lee, J. Park, Y. Chung, H.B. Na, J. Am. Chem. Soc. **123**, 12798 (2001).
[12] L. I. Berger, Semiconductor Materials, CRC Press, Boca Raton, FL. (1997)
[13] J. Tauc, R. Grigorovici, A. Vancu, Phys. Status Solidi. **15**, 627 (1966).
[14] M. H. Huang, Y. Wu, H. Feick, N. Tran, E. Weber, P. Yang, Advanced Materials. **13**, 113 (2001).
[15] J. Zhou, F. Zhao, Y. Wang, Y. Zhang, L. Yang, Journal of Luminescence. **122**, 195 (2007).
[16] G. Williams, P. V. Kamat, Langmuir. **25**, 13869 (2009).
[17] Z-P. Sun, L. Liu, L. Zhang, D. Z. Jia, Nanaotechnology. **17**, 2266 (2006).
[18] Z. Peng, X. Peng, J. Am. Chem. Soc. **124**, 3343 (2002).
[19] X. G. Peng, L. Manna, W. D. Yang, J. Wickham, E. Scher, A. Kandavich, A. P. Alivisatos, Nature. **404**, 59 (2000).